Water Catalysis in Radical Reactions

Artur Mardyukov

Hydroxyl Radical

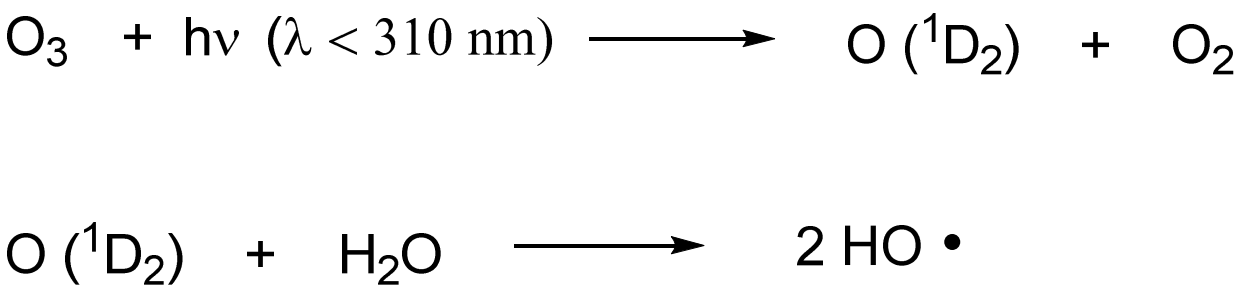

Sasho Gligorovski, Rafal Strekowski, Stephane Barbati, and Davide, *Chem. Rev* , **2015**, 115, 13051-13092.

Criegee Intermediate / X-Factor

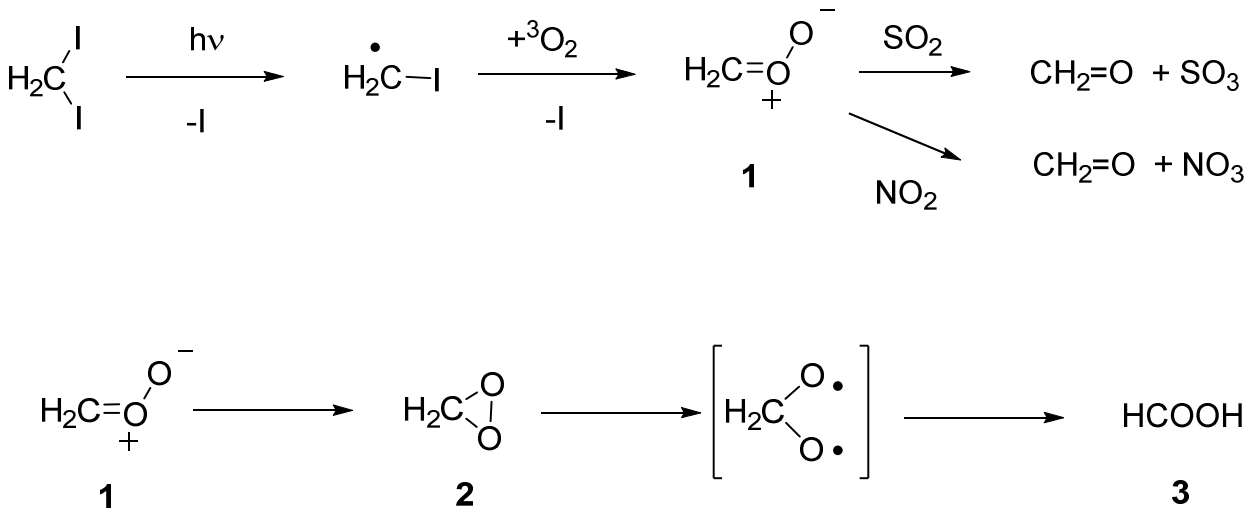

Mass Selected Photoionization Spectroscopy - 2 ms.

(1) O. Welz, J. D. Savee, D. L. Osborn, S. S. Vasu, C. J. Percival, D. E. Shallcross, C. A. Taatjes, Science **2012**, 335, 204 – 207 (2) C. A. Taatjes, O. Welz, A. J. Eskola, J. D. Savee, A. M. Scheer, D. E. Shallcross, B. Rotavera, E. P. F. Lee, J. M. Dyke, D. K. W. Mok, D. L. Osborn, C. J. Percival, Science **2013**, 340, 177 – 180. (3) Wen Chao, Jun-Ting Hsieh, Chun-Hung Chang, Jim Jr-Min Lin, *Science* , **2015**, 347, 6223. (4) Mauldin, R. L. *et al. Nature* **488,** 193–196 (**2012**).

Criegee Intermediate – IR Spectrum

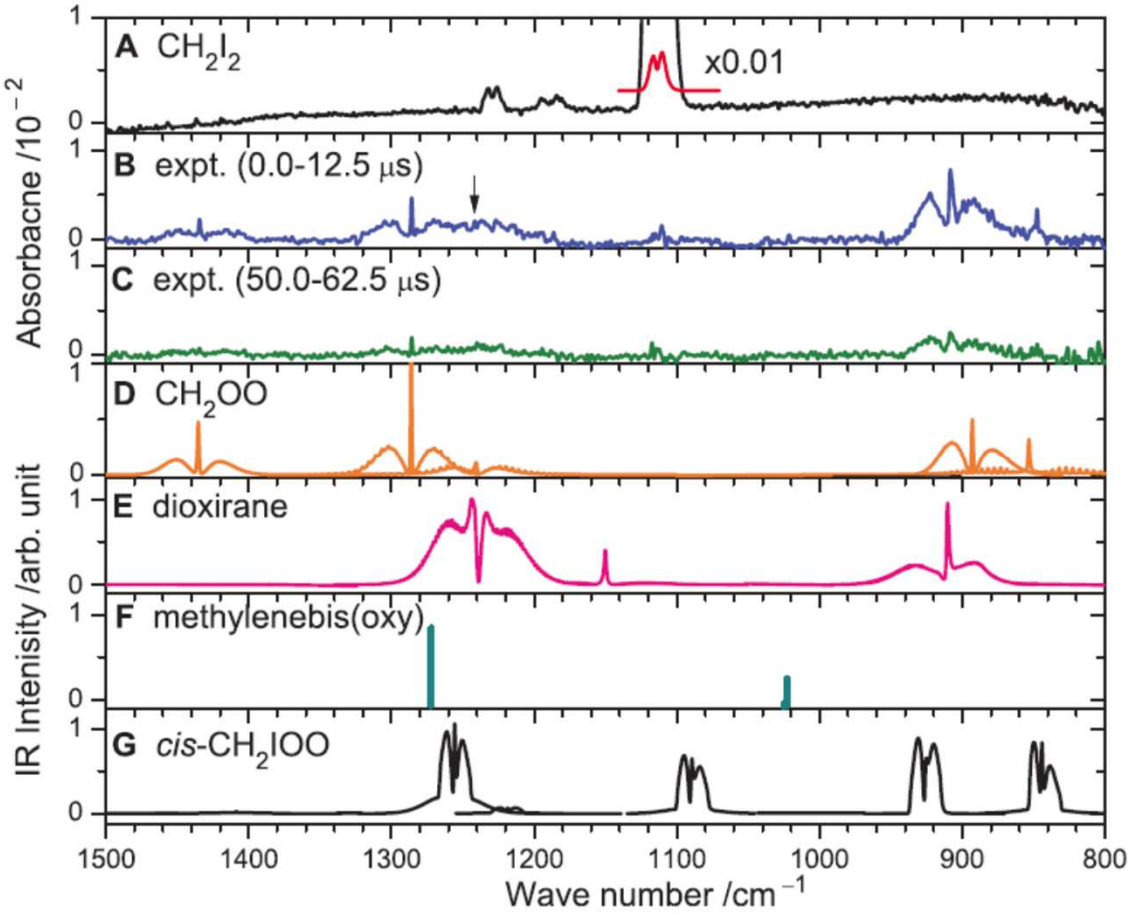

Yu-Te Su, Yu-Hsuan Huang, Henryk A. Witek, Yuan-Pern Lee, *Science* , **2013**, 340, 174.

Criegee Intermediate

ATMOSPHERIC CHEMISTRY

Direct kinetic measurement of the reaction of the simplest Criegee intermediate with water vapor

Wen Chao,[1,2] Jun-Ting Hsieh,[1,3] Chun-Hung Chang,[1] Jim Jr-Min Lin[1,2,4]*

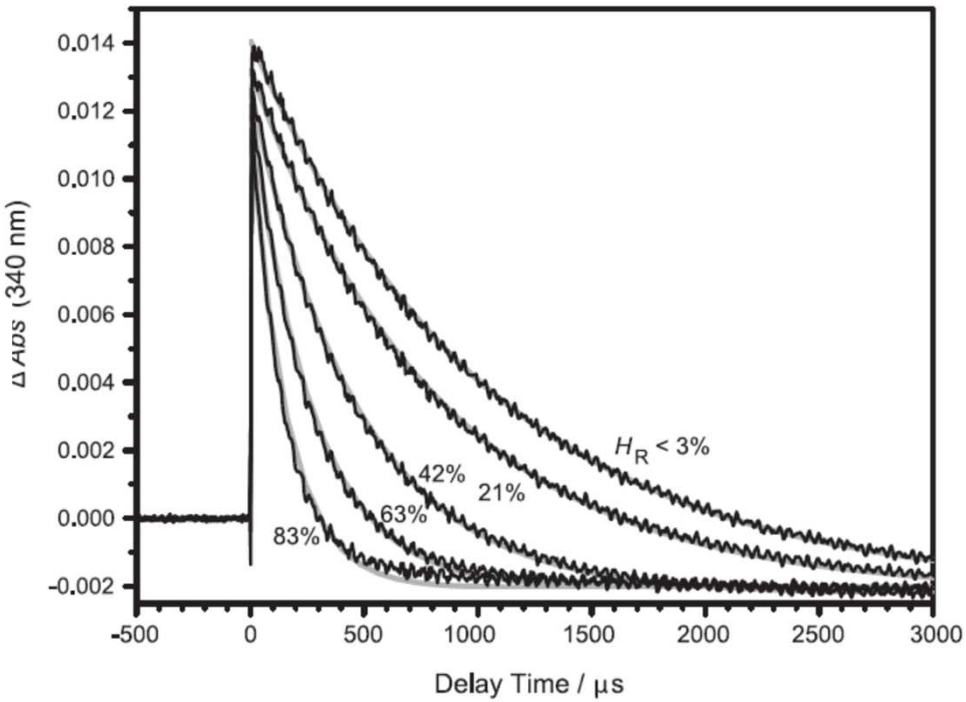

Typical temporal profiles of the absorbance change near the peak of the CH_2OO band.The smooth lines are single-exponential fits to the experimental data, which were averaged for 60 to 120 laser shots. Because IO absorbs rather weakly in this wavelength window and the depletion of CH_2I_2 is constant after the photolysis (causing negative baselines at long times), these temporal profiles mainly represent changes in [CH_2OO].

Wen Chao, Jun-Ting Hsieh, Chun-Hung Chang, Jim Jr-Min Lin, *Science* , **2015**, 345, 751.

Water Catalysis of a Radical-Molecule Gas-Phase Reaction

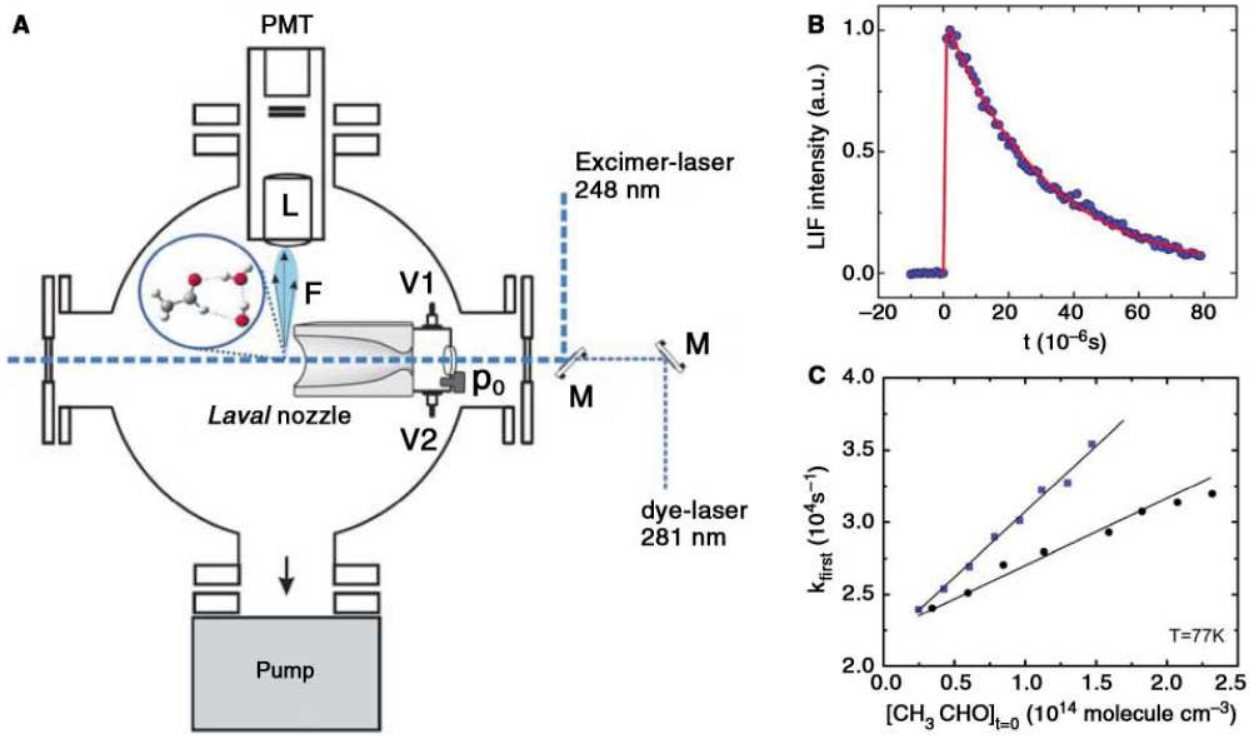

(A) Laval nozzle expansion apparatus used here. p_0 represents the pressure in front of the Laval nozzle; V1 and V2, valves feeding the nozzle reservoir; F, fluorescence; L, lens system for the collection of fluorescence; M, mirrors; and PMT, photomultiplier. (B) LIF profiles of OH in the reaction between acetaldehyde and OH radicals (T = 77 K, $\rho_{tot} = 8.5 \times 10^{16}$ molecule cm^{-3}, ρ aldehyde = 1.6×10^{14} molecule cm^{-3}, ρOH ≈ 1.5×10^{11} molecule cm^{-3}). (C) Pseudo-first-order rate constants k as a function of acetaldehyde concentration (buffer gas N_2, T = 77 K, $\rho_{to}t = 8.5 \times 10^{16}$ molecule cm^{-3}). Circles, reaction without water; squares, reaction with water (single experiments).

E. Vöhringer-Martinez, B. Hansmann, H. Hernandez, J. S. Francisco, J. Troe, B. Abel, *Science* , **2007**, 315, 497.

Water Catalysis of a Radical-Molecule Gas-Phase Reaction

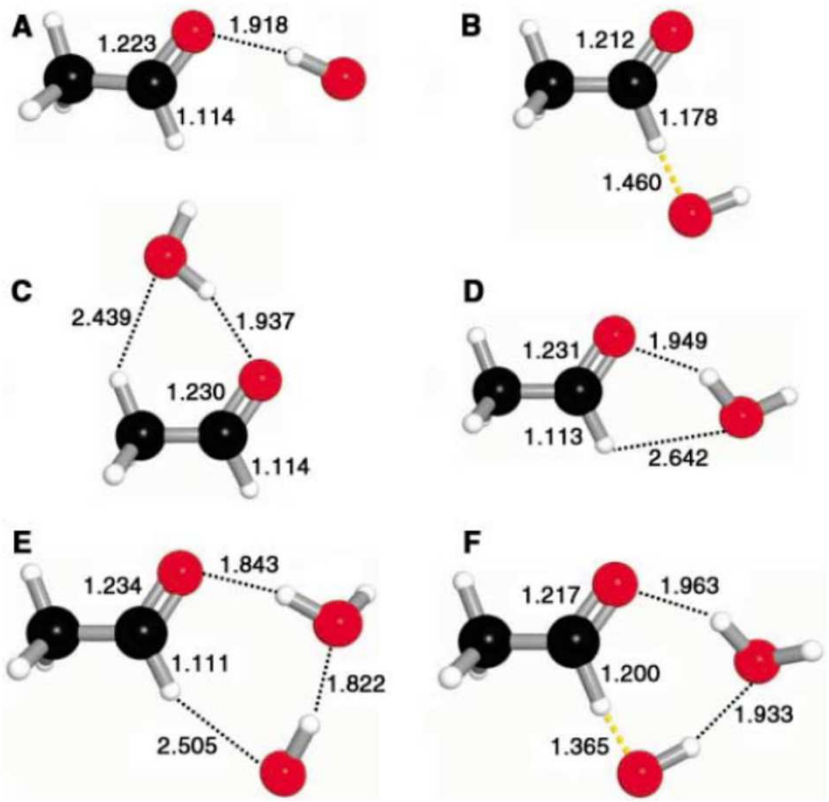

Calculated structures (A to F) of reactant complexes, prereaction compexes, and transition states. Structures (bond lengths in Å) are at characteristic points along the reaction coordinates using the MP2 level of theory with the aug-cc-pVDZ basis set. (A) and (B) are the prereaction complex and the transition state without water, respectively. (C) and (D) are prospective water-acetaldehyde clusters from which (D) was identified to be relevant for the reaction. (E) is the prereaction complex, and (F) is the transition state for the reaction in the presence of water.

E. Vöhringer-Martinez, B. Hansmann, H. Hernandez, J. S. Francisco, J. Troe, B. Abel, *Science* , **2007**, 315, 497.

Water Catalysis of a Radical-Molecule Gas-Phase Reaction

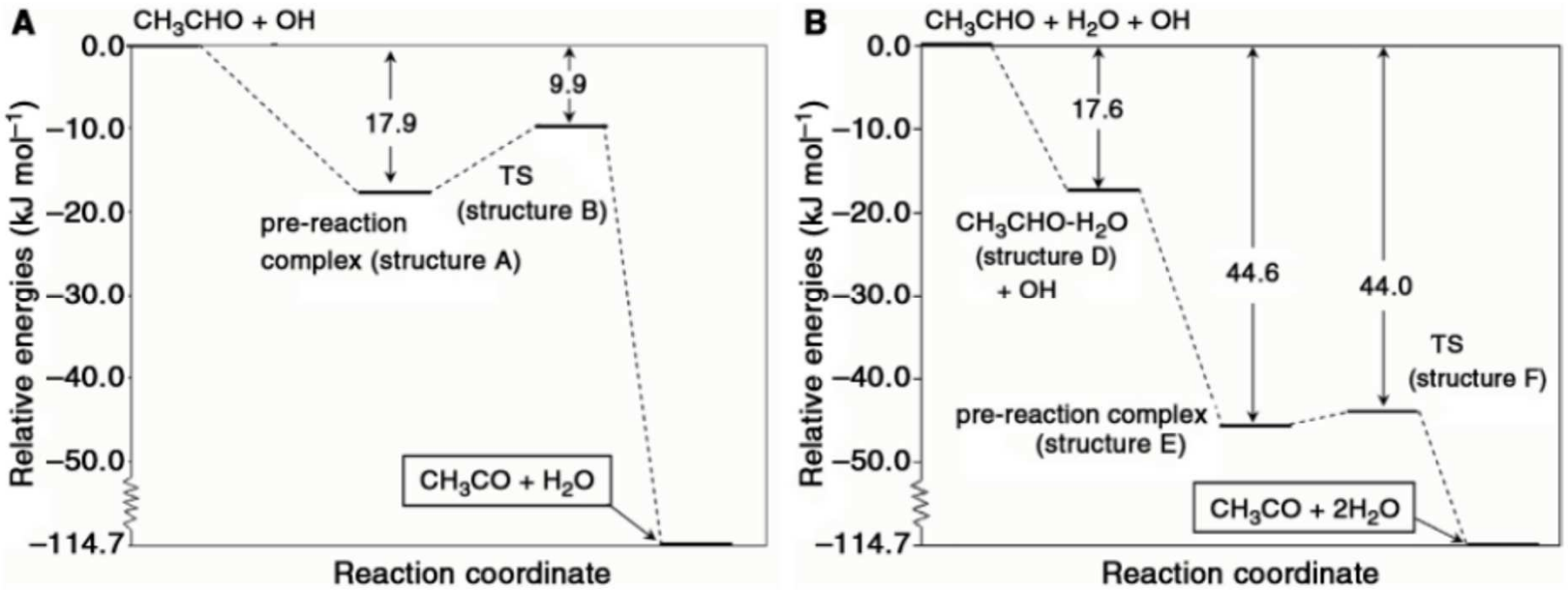

Relative energies for the reaction in the absence (A) and the presence (B) of water. The energies are calculated at the CCSD(T) level of theory with the correlation consistent polarized triple zeta (cc-VTZ) basis set.

E. Vöhringer-Martinez, B. Hansmann, H. Hernandez, J. S. Francisco, J. Troe, B. Abel, *Science* , **2007**, 315, 497.

Switching on the fluorescence of 2-aminopurine by site-selective microhydration

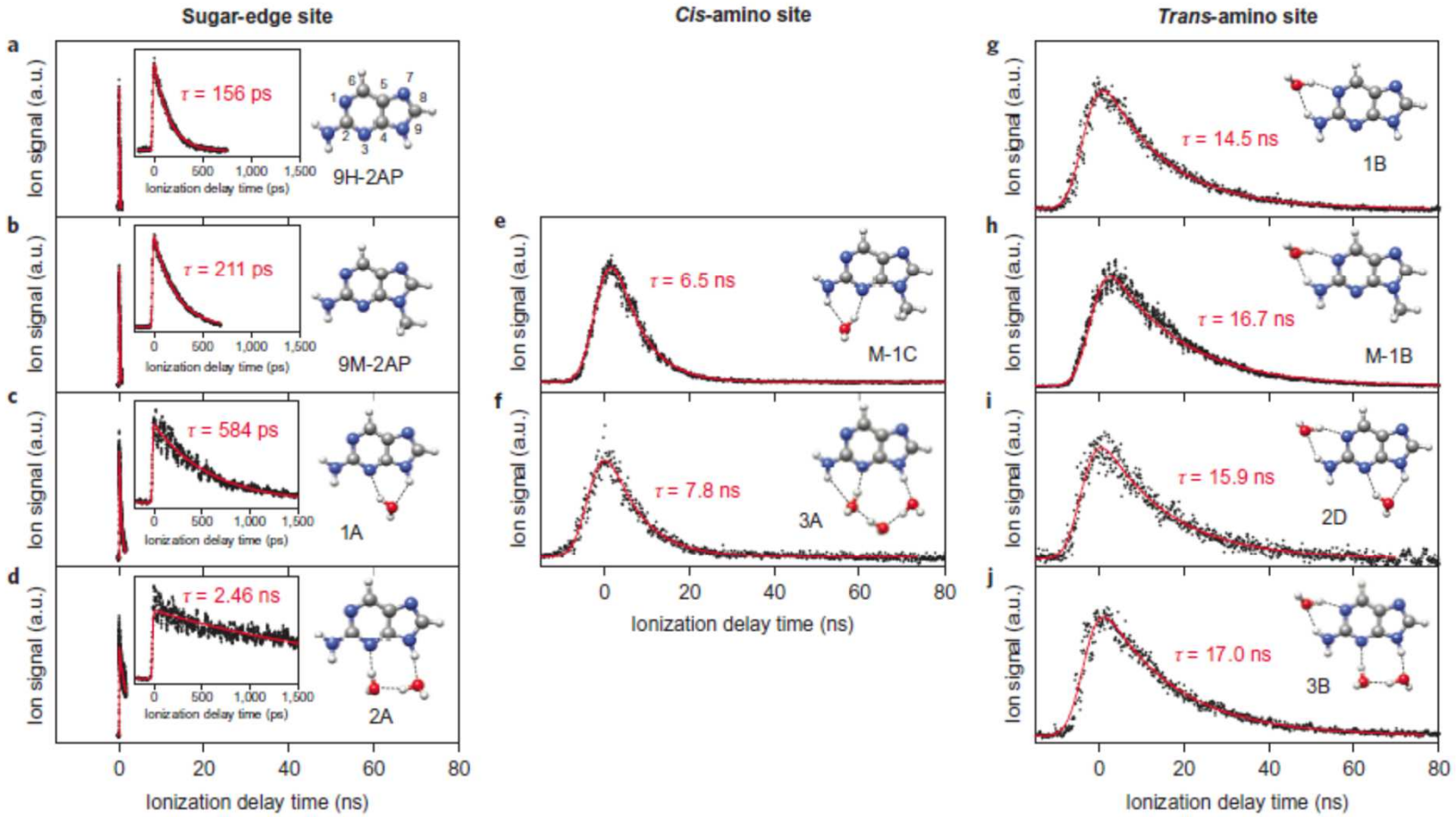

Simon Lobsiger, Susan Blaser, Rajeev K. Sinha, Hans-Martin Frey and Samuel Leutwyler, *Nat. Chem.*, **2014**, 989.

Switching on the fluorescence of 2-aminopurine by site-selective microhydration

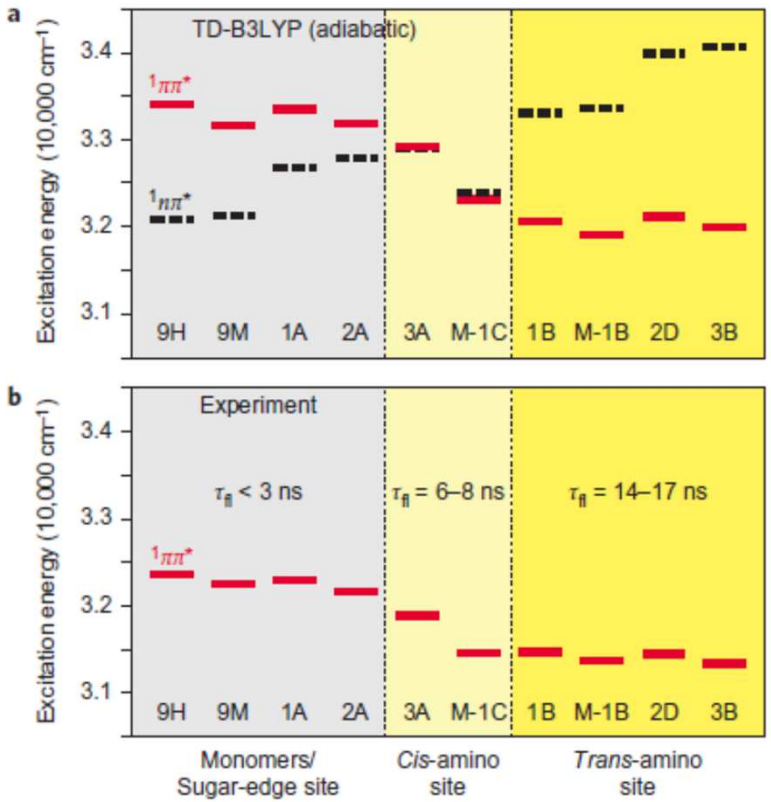

Energies (in cm^{-1}) are shown for 9H-2AP (9H), 9M-2AP (9M) and their mono-, di- and trihydrate clusters (1A to 3B). The labels of the different species are defined in Fig. 1a–j. The background colour qualitatively indicates the fluorescence lifetime. a, Calculated time dependent DFT (B3LYP/TZVP) adiabatic energies of the 1ππ* (full red lines) and 1nπ* states (black dashed lines). b, Experimental 1ππ* adiabatic transition energies of the respective supersonic-jet-cooled molecules and clusters, measured by R2PI spectroscopy.

Simon Lobsiger, Susan Blaser, Rajeev K. Sinha, Hans-Martin Frey and Samuel Leutwyler, *Nat. Chem.*, **2014**, 989.

Atmospheric Chemistry | *Hot Paper*

International Edition: DOI: 10.1002/anie.201509311
German Edition: DOI: 10.1002/ange.201509311

Red-Light-Induced Decomposition of an Organic Peroxy Radical: A New Source of the HO_2 Radical

*Manoj Kumar and Joseph S. Francisco**

Abstract: *The gas-phase decomposition of the α-hydroxy methylperoxy radical has been theoretically examined, and the results provide insight into a new source of the hydroperoxy radical (HO_2) in the troposphere. Bimolecular peroxy decomposition is promoted by the red-light or near-IR radiation excitation. The calculations suggest for the first time, an important chemical role for the $H_2O{\cdot}HO_2$ radical complex that exist in significant abundance in the troposphere. In particular, the reaction of organic peroxy radicals with the HO_2 radical and the $H_2O{\cdot}HO_2$ radical complex represent an autocatalytic source of atmospheric HO_2. This reaction is a new example of red-light-initiated atmospheric chemistry that may help in understanding the discrepancy between the observed and measured levels of the HO_x at sunrise.*

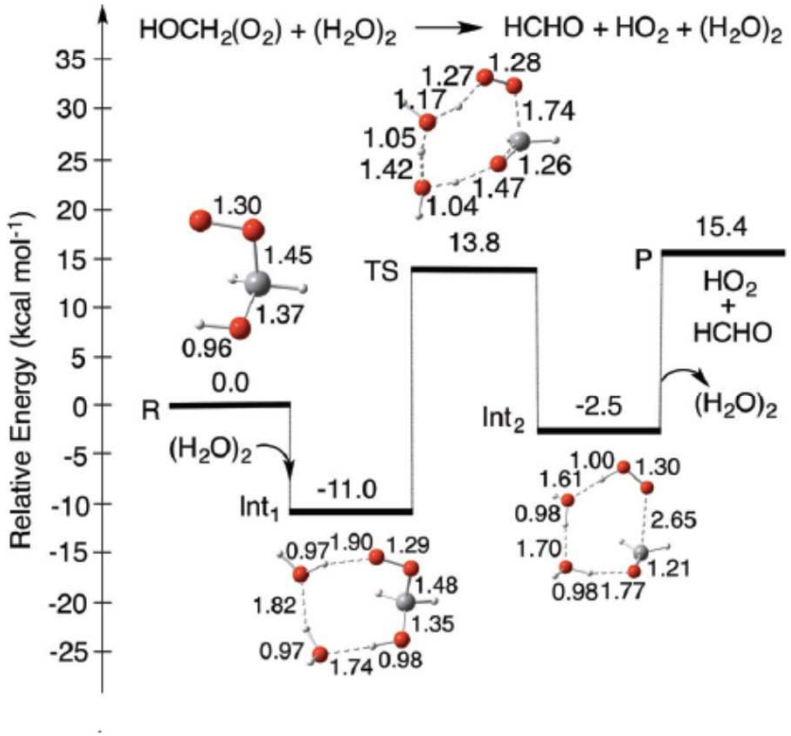

Phenylperoxy Radical

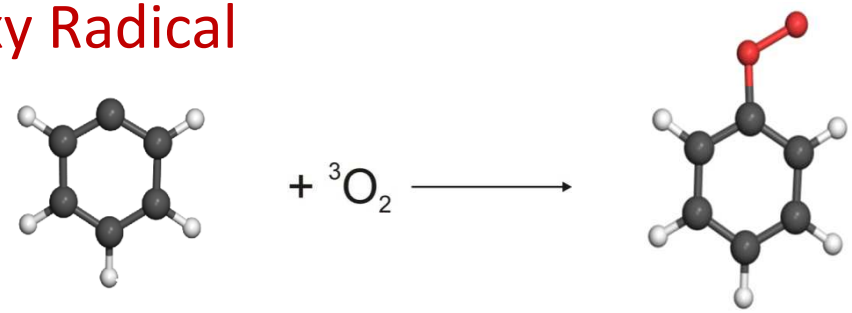

$\Delta G = -46.3$ *kcal/mol* (UB3LYP/6-311++G(2d,2p))

The symmetry point group of ***phenyl peroxy*** **radical** *is the* C_s *and* $^2A''$ *is the electronic ground state*.

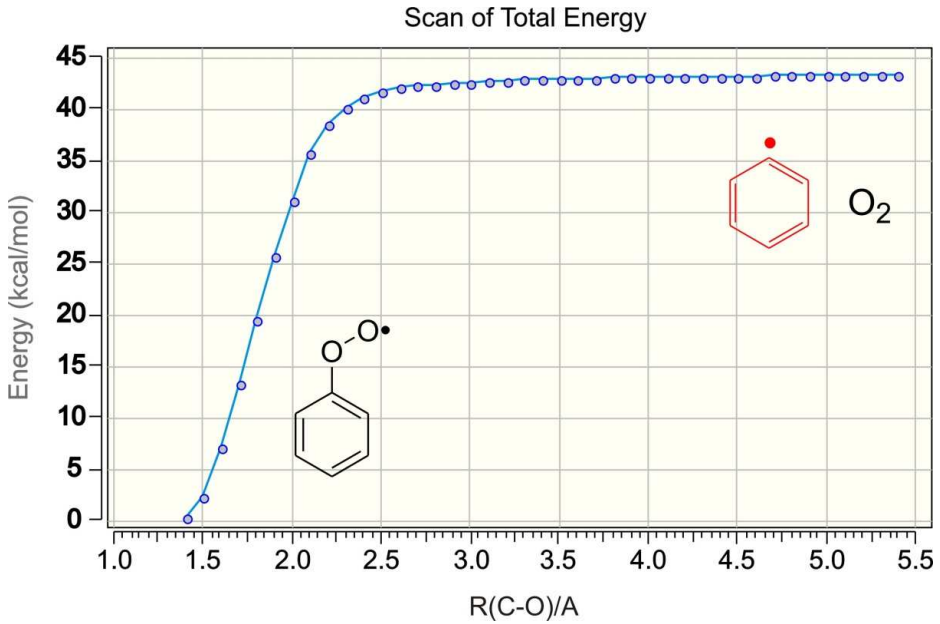

The phenyl peroxy radical potential energy profile calculated at the UB3LYP/6-311++G(2d,2p) level of theory.

J. Phys. Chem. A, **2005**, 15, 6114

The Reaction of Phenyl Radical with Molecular Oxygen: A G2M Study of the Potential Energy Surface

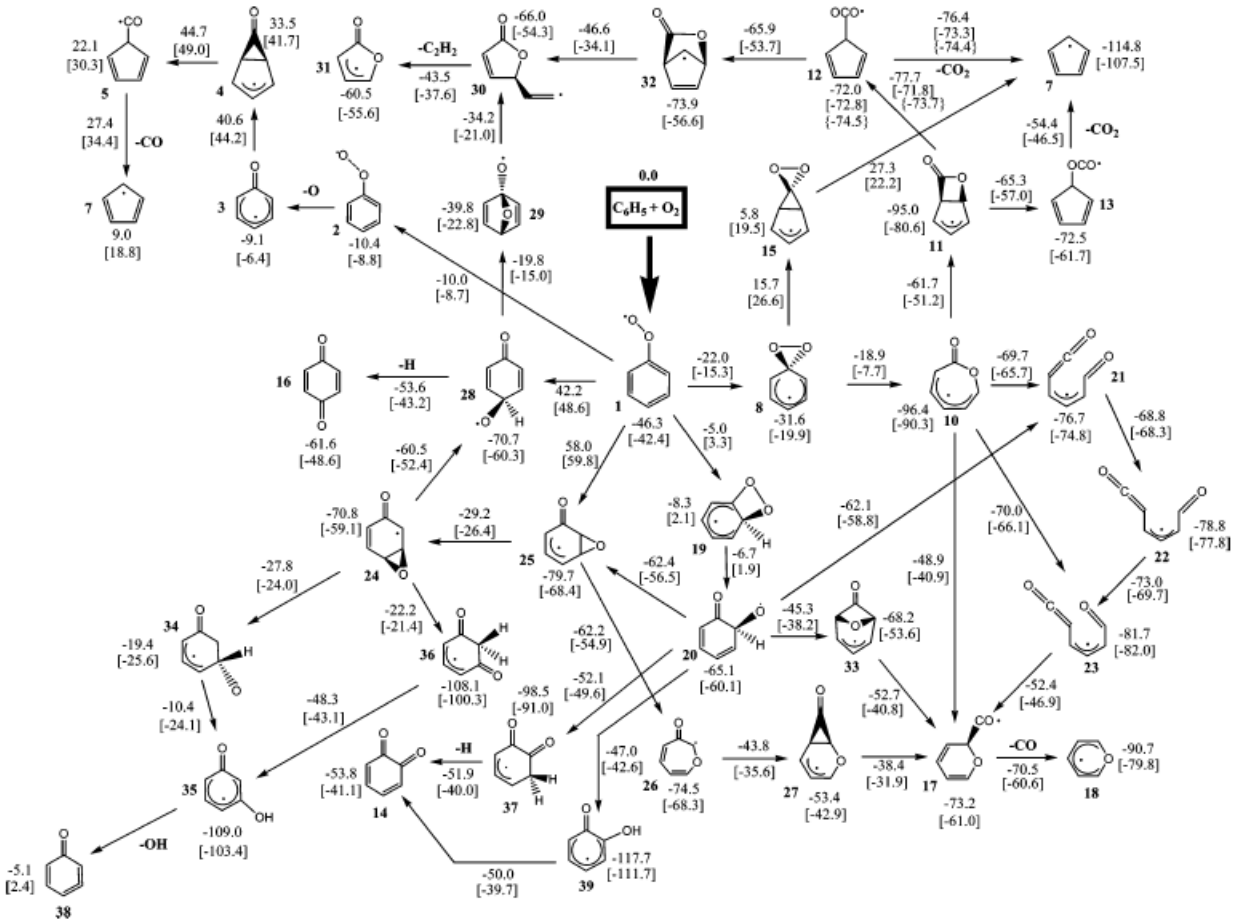

A graph of possible pathways on the global potential energy surface of the C6H5 + O2 reaction. Relative energies of the reactants, products, intermediates, and transition states are given in kcal/mol as calculated at the G2M and B3LYP/6-311++G** (in brackets) levels.

Igor V. Tokmakov, Gap-Sue Kim, Vadim V. Kislov, Alexander M. Mebel, Ming C. Lin, *JPCA*, **2005**, 109, 6114.

Synthesis of Phenylperoxy Radical

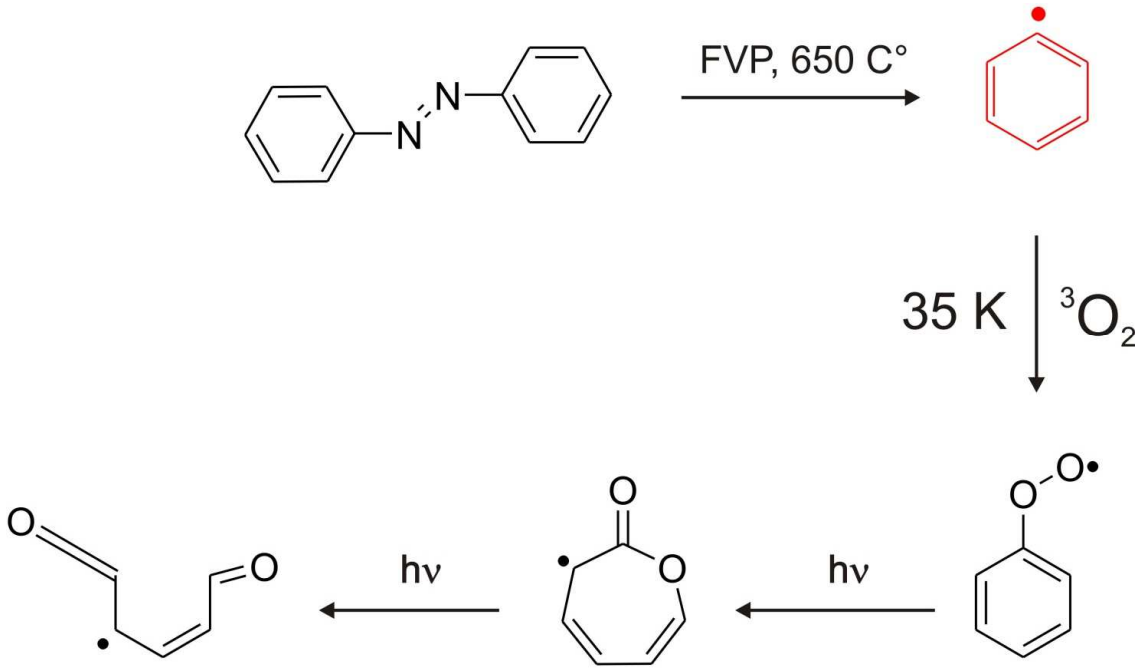

Artur Mardyukov, Wolfram Sander, *Chem. Eur*. J. **2009**, 15, 1462-1467.

Synthesis of Phenylperoxy Radical

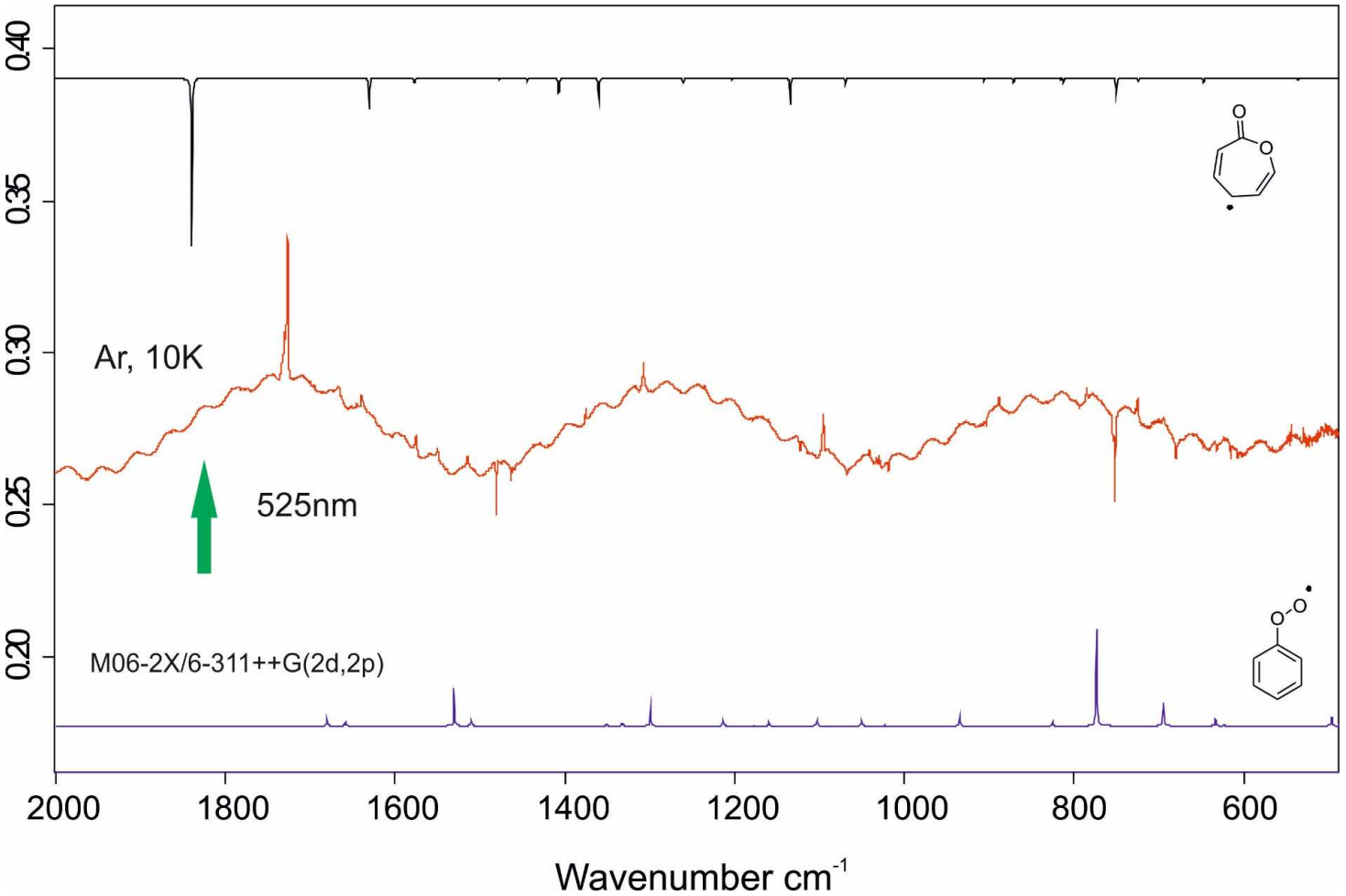

Phenylperoxy Radical

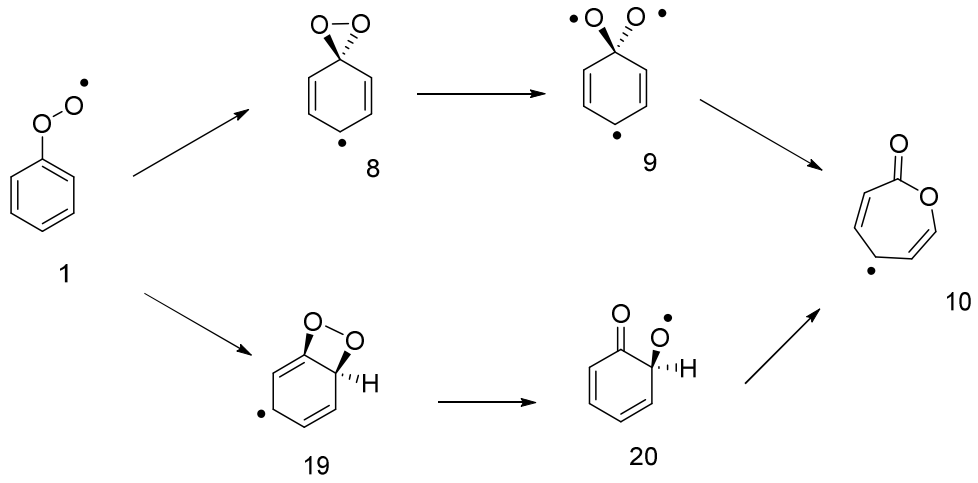

A possible pathways on the potential energy surface of phenylperoxy radical

(1) Igor V. Tokmakov, Gap-Sue Kim, Vadim V. Kislov, Alexander M. Mebel, and Ming C. Lin, *J. Phys. Chem. A* **2005,** *109,* 6114-6127. (2) Cynthia Barckholtz, Michael J. Fadden, and Christopher M. Hadad, *J. Phys. Chem. A* **1999,** *103,* 8108-8117. (3) Michael J. Fadden, Cynthia Barckholtz, and Christopher M. Hadad, *J. Phys. Chem. A* **2000,** *104,* 3004-3011. (4) Michael J. Fadden and Christopher M. Hadad, J. Phys. Chem. A 2000, 104, 8121-8130. (5) Barry K. Carpenter, *J. Am. Chem. Soc. 1993,*115**.** 9806-9807.

Phenylperoxy – Water Complexes

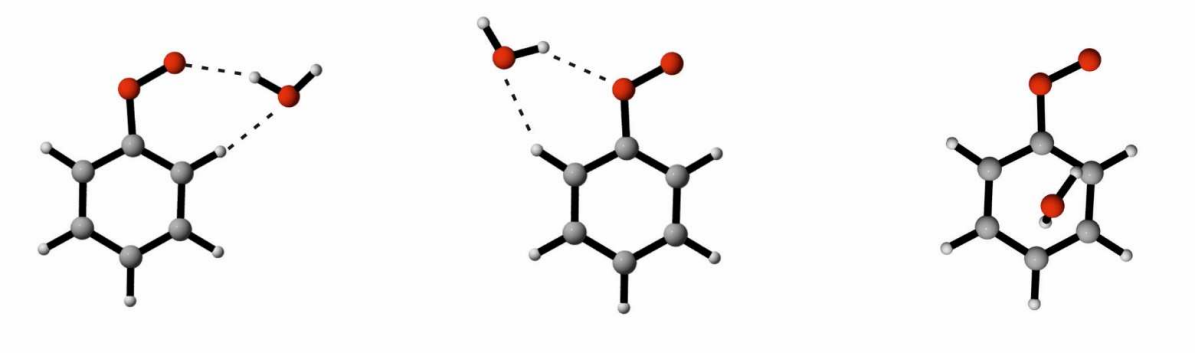

1a (-2.95 / -2.36) **1b** (-3.00 / -2.31) **1c** (-2.43 / -1.74**)**

M06-2X/6-311++G(2d,2p)
B3LYP/6-311++G(2d,2p)

Spin Density

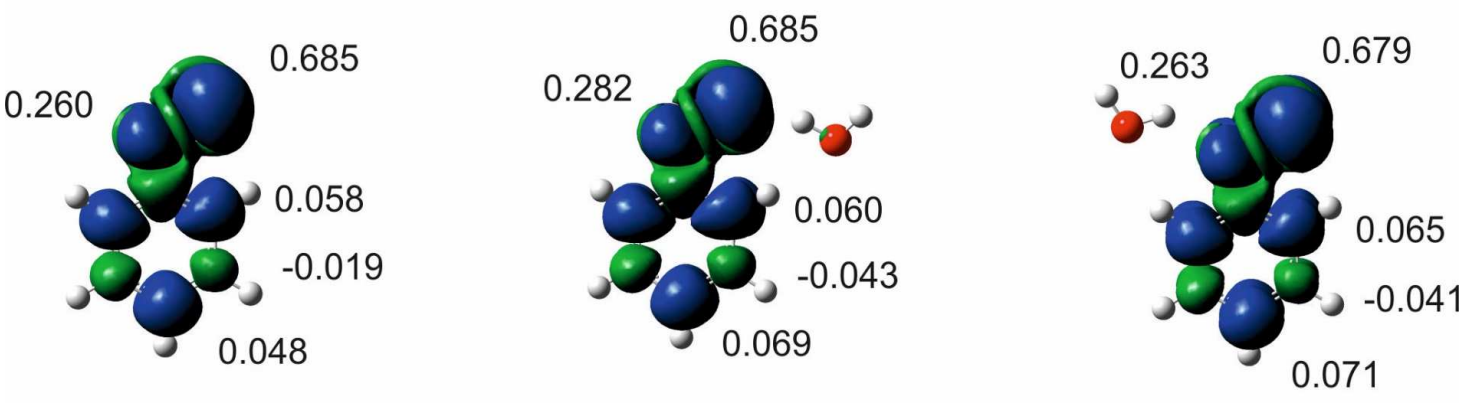

Phenylperoxy – Water Complexes

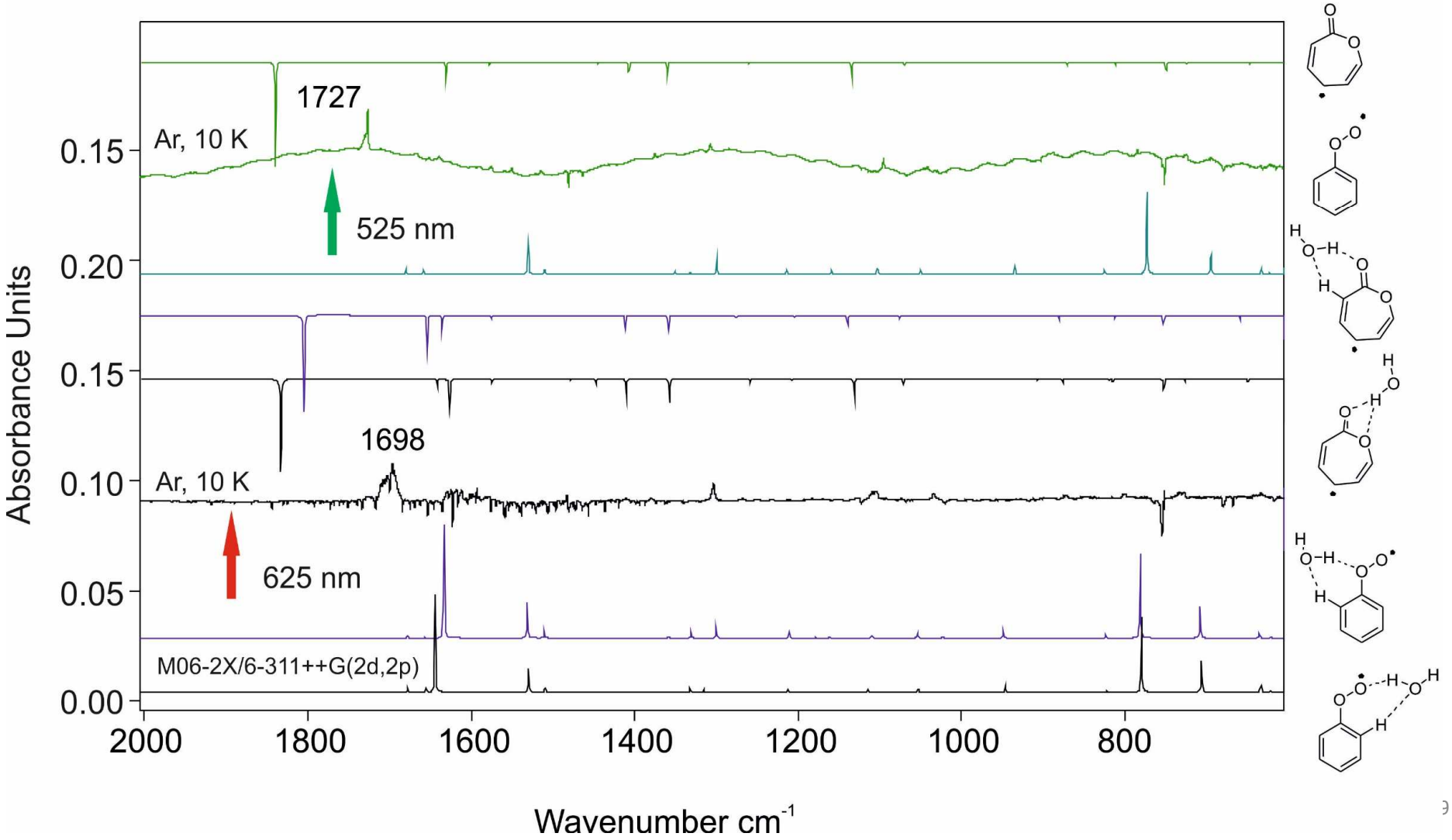

Photochemistry

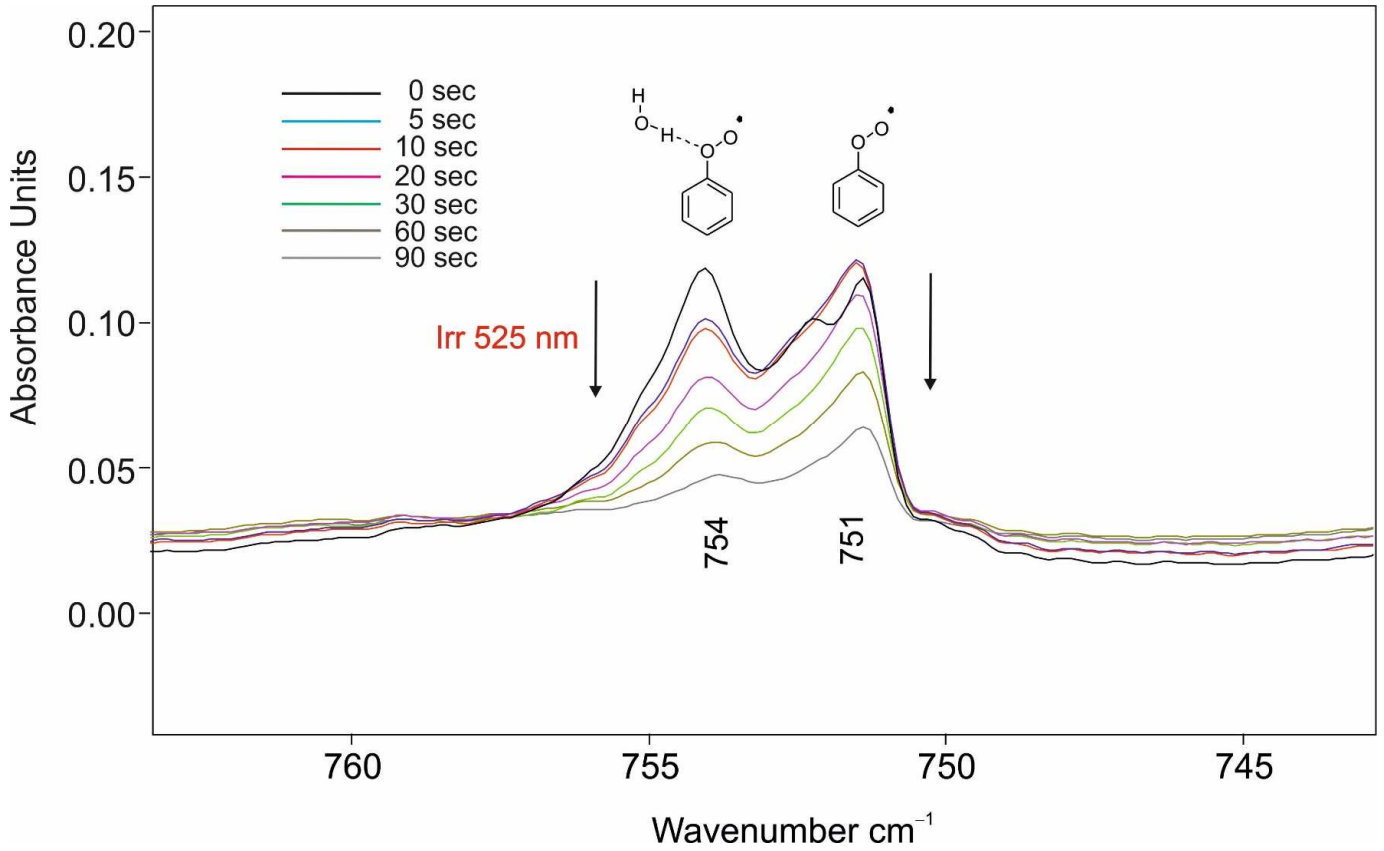

Disappearance of the IR bands of both phenylperoxy radical and phenylperoxy radical – water complex at 754 and 751 cm^{-1} after irradiation with light $\lambda = 525$ nm in an argon matrix at 10 K.

Photochemistry

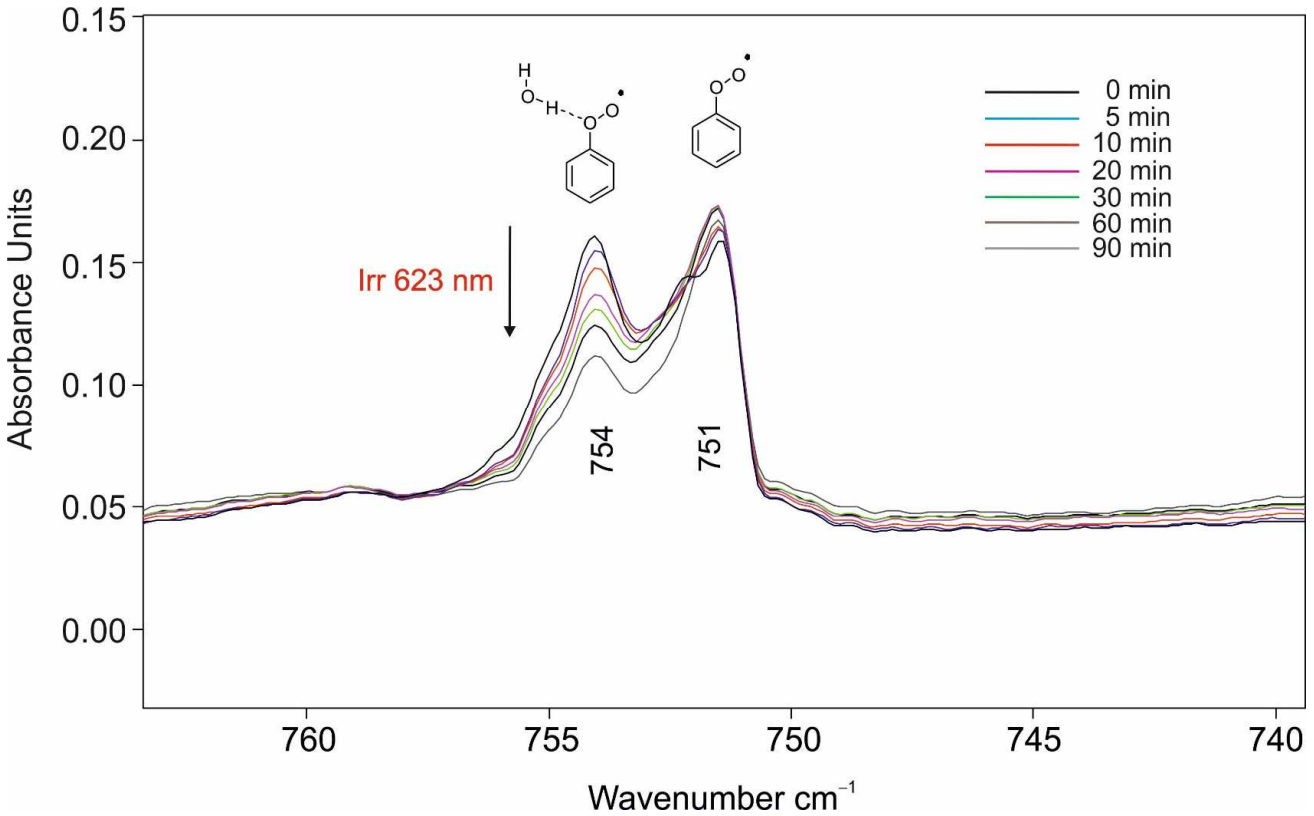

Disappearance of the IR band of phenylperoxy radical – water complex at 754 cm^{-1} after irradiation with light λ = 623 nm in an argon matrix at 10 K, whereas the IR band of phenylperoxy radical at 751 cm^{-1} remains unchanged upon irradiation.

Phenylperoxy Radical – Water

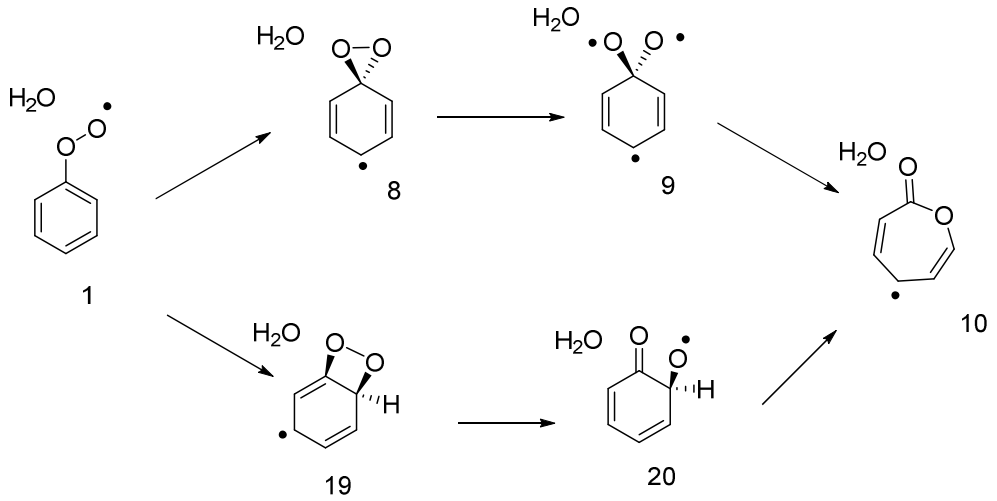

Phenylperoxy Radical – PES

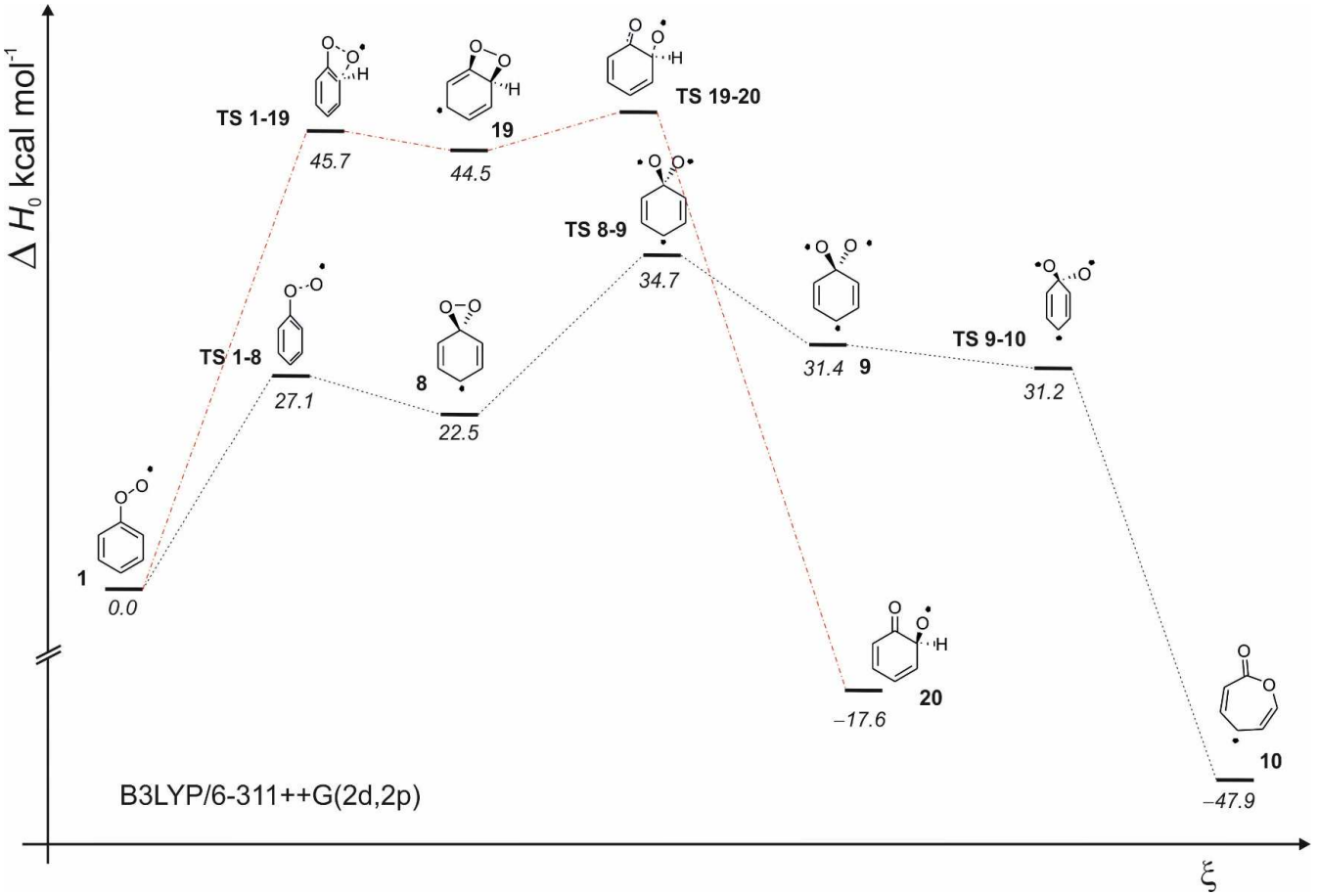

Phenylperoxy Radical – Water: PES

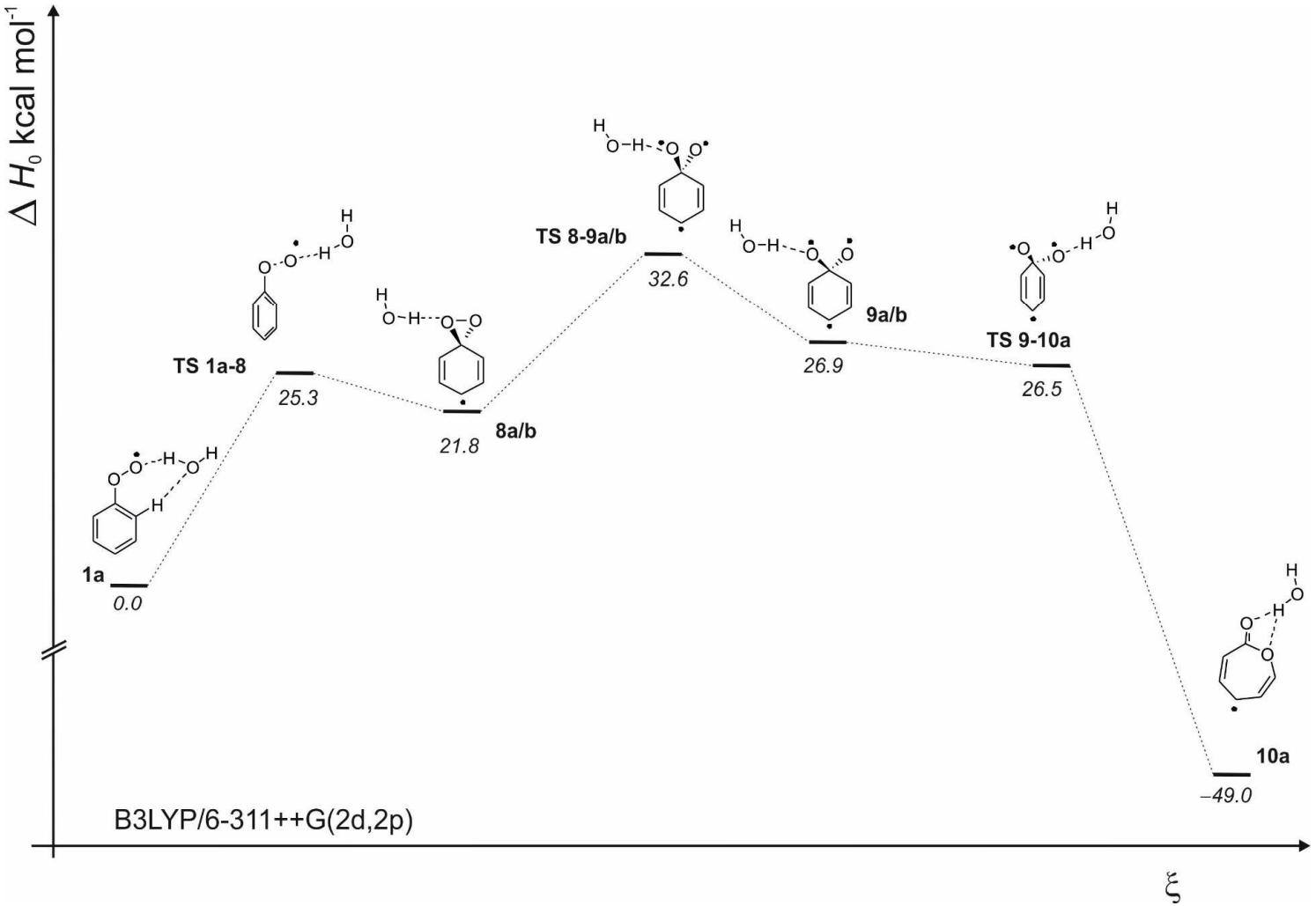

Phenylperoxy Radical – Water: PES

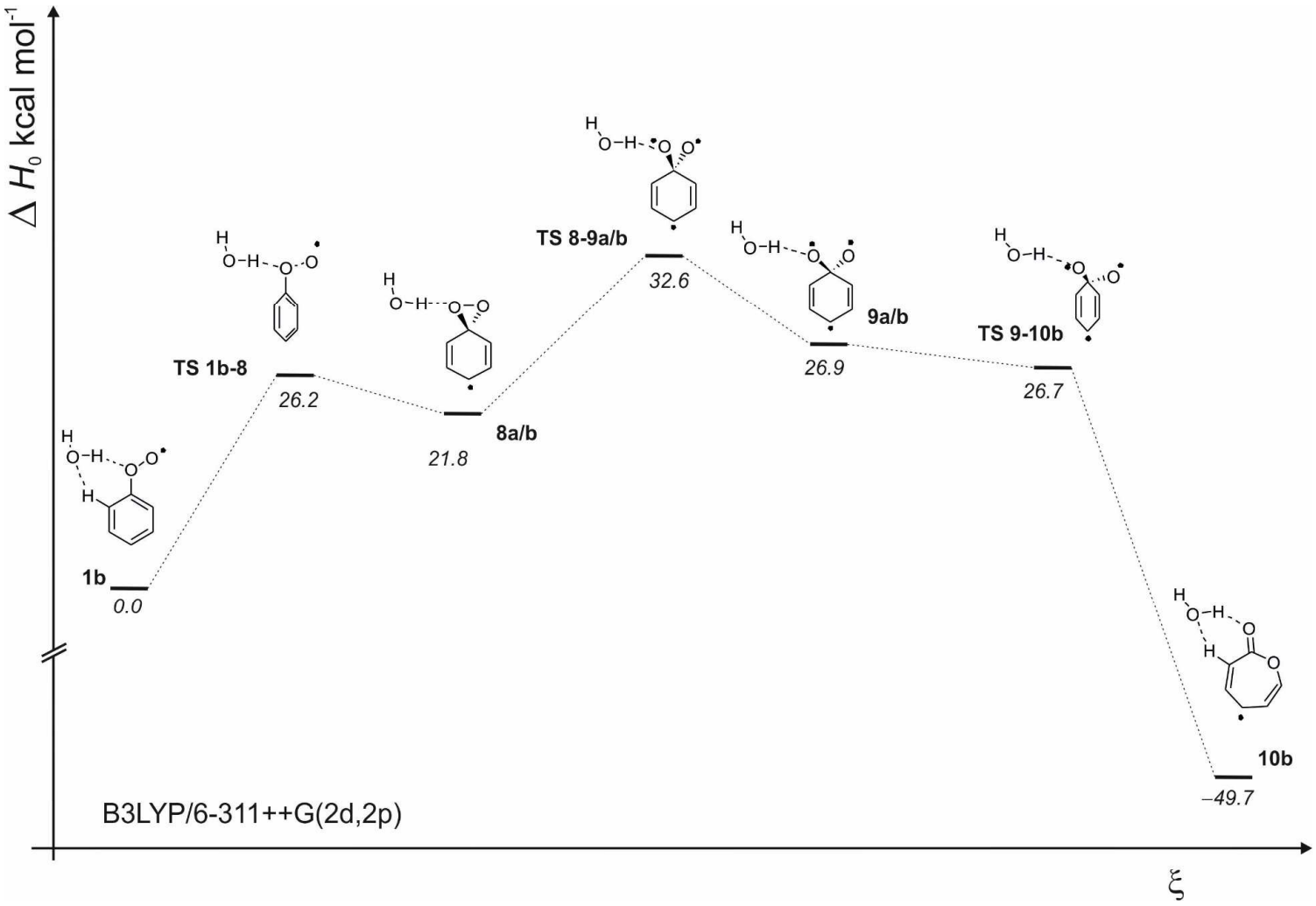

Photochemistry of Phenylperoxy Radical and Phenylperoxy Radical – Water Systems

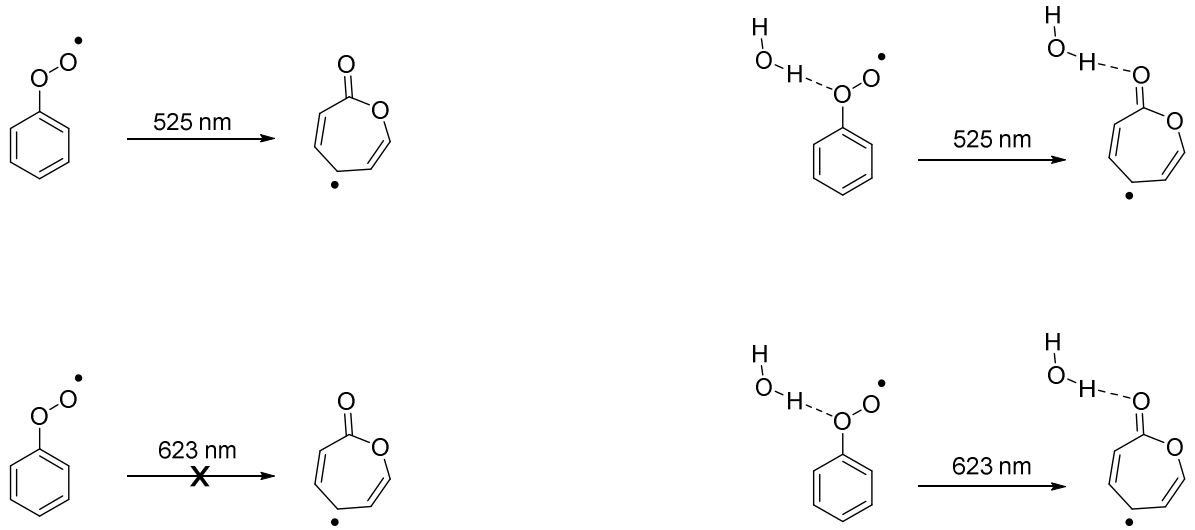

- Water as Catalyst
- Energy upconversion
- Overtone-induced process

Trifluoromethylhydroxycarbene: Conformer-Specific Hydrogen Atom Tunneling

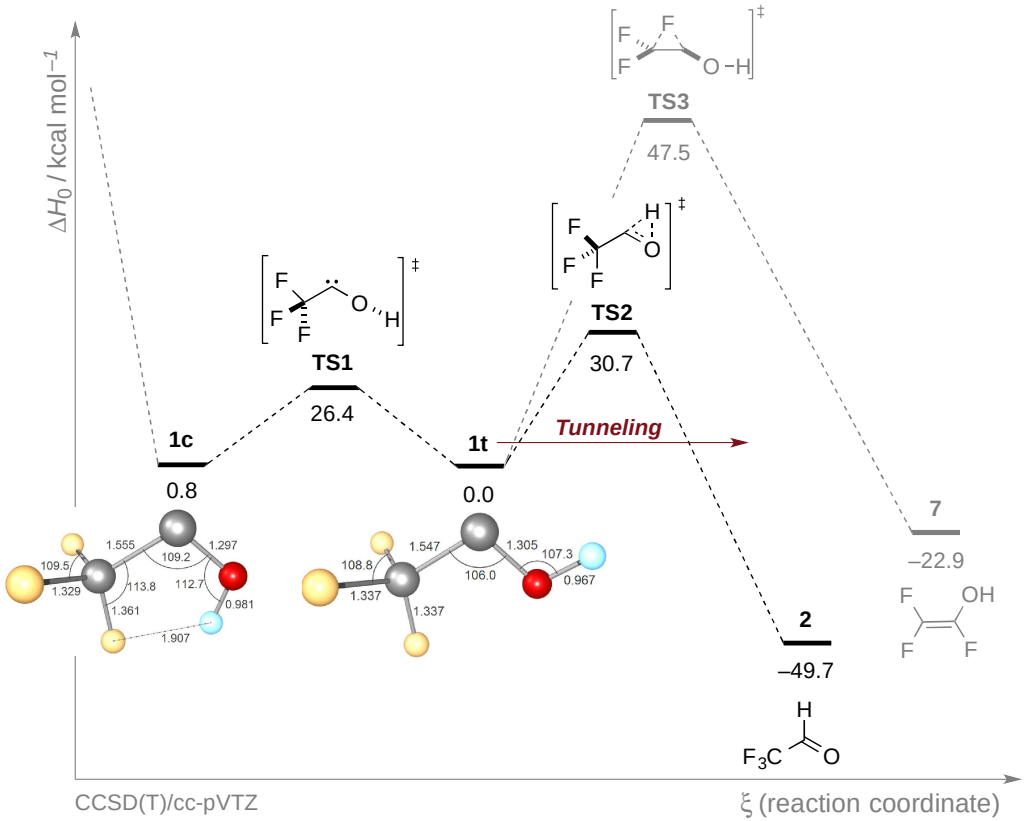

Mardyukov, Quanz, Schreiner, *Nat. Chem.*, **2016**, accepted.

Microhydration of Trifluoromethylhydroxycarbene

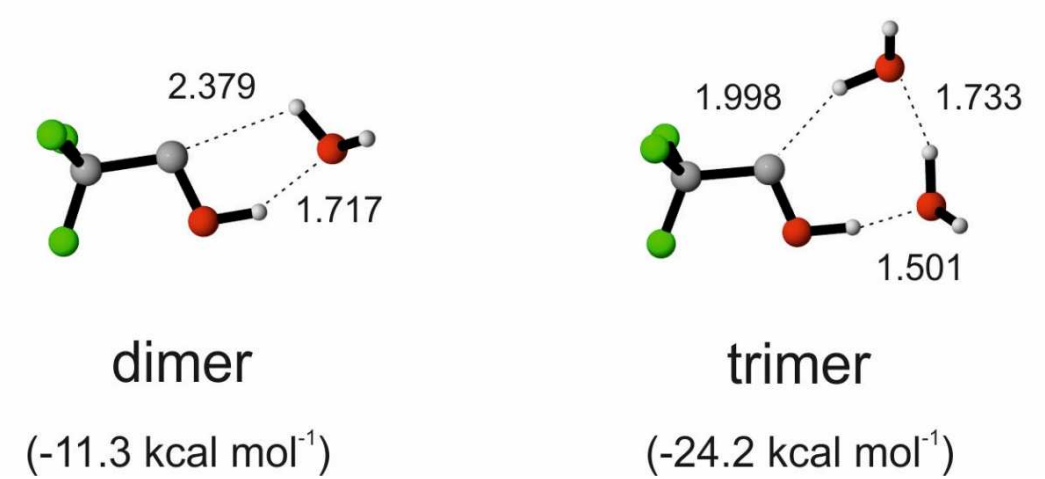

M06-2X/6-311++G(2d,2p)

Trifluoromethylhydroxycarbene – Water

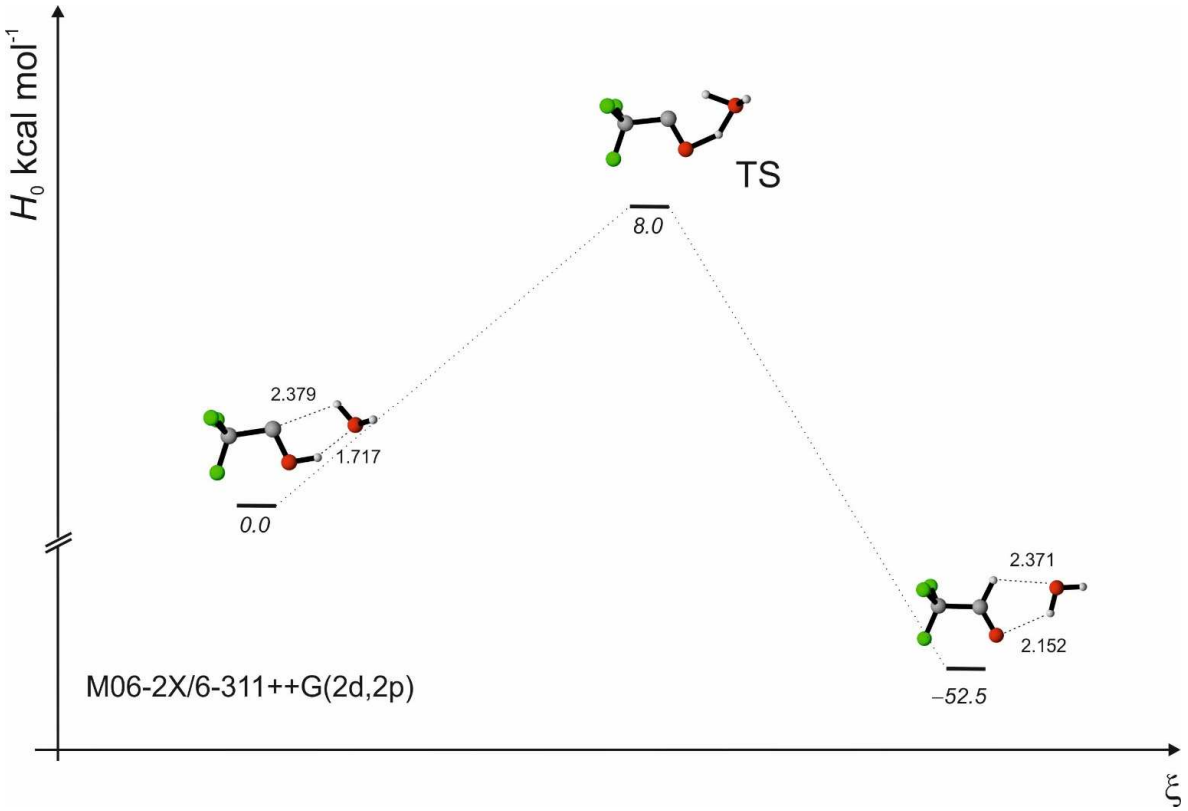

Trifluoromethylhydroxycarbene – 2Water

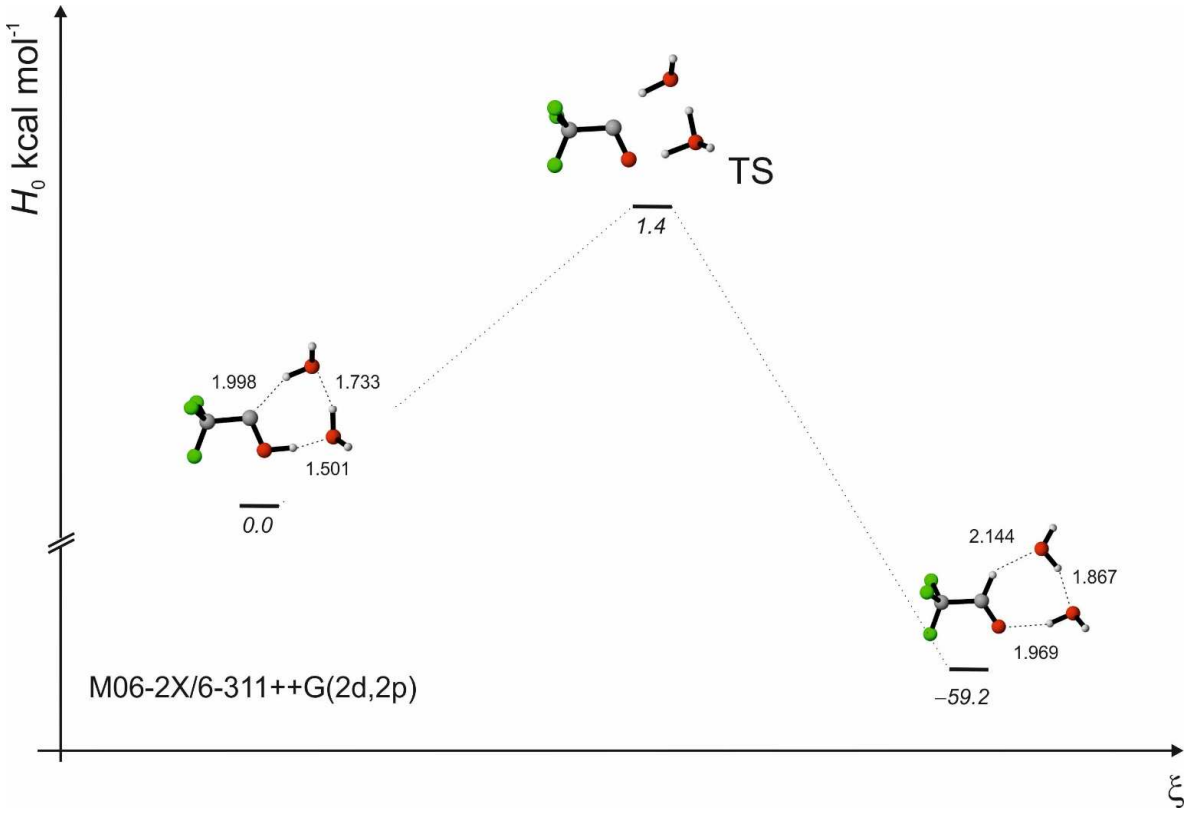

Contrasting Effects of Water on the Barriers to Decarboxylation of Two Oxalic Acid Monohydrates: A Combined Rotational Spectroscopic and Ab Initio Study

Elijah G. Schnitzler, Courtenay Badran, and Wolfgang Jäger*

Department of Chemistry, University of Alberta, Edmonton, Alberta T6G 2G2, Canada

Supporting Information

ABSTRACT: Using rotational spectroscopy, we have observed two isomers of the monohydrate of oxalic acid, the most abundant dicarboxylic acid in the atmosphere. In the lowest-energy isomer, water hydrogen-bonds to both carboxylic acid groups, and the barrier to decarboxylation decreases. In the second isomer, water bonds to only one carboxylic acid group, and the barrier increases. Though the lower barrier in the former is not unequivocal evidence that water acts as a photocatalyst, the higher barrier in the latter indicates that water acts as an inhibitor in this topology. Oxalic acid is unique among dicarboxylic acids: for the higher homologues calculated, the inhibiting topology of the monohydrate is lowest in energy and most abundant under atmospheric conditions. Consequently, oxalic acid is the only dicarboxylic acid for which single-water catalysis of overtone-induced decarboxylation in the atmosphere is plausible.

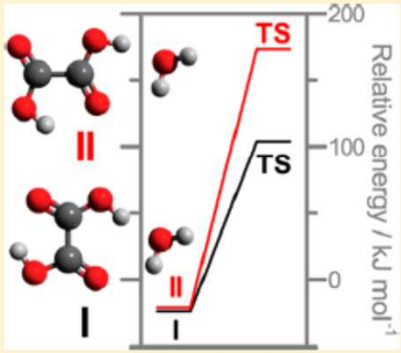

J. Phys. Chem. Lett, **2016**, 7, 1143-1147.

Acknowledgements

Prof. Dr. Peter R. Schreiner

PRS Group

nature chemistry

ARTICLES

PUBLISHED ONLINE: 4 APRIL 2016 | DOI: 10.1038/NCHEM.2488

Unimolecular dissociation dynamics of vibrationally activated CH_3CHOO Criegee intermediates to OH radical products

Nathanael M. Kidwell[1†], Hongwei Li[1†], Xiaohong Wang[2†], Joel M. Bowman[2*] and Marsha I. Lester[1*]

The hydroxyl radical is an important atmospheric oxidant, and a significant source of its production occurs through alkene ozonolysis. This takes place via a cycloaddition reaction and subsequent fragmentation to form an energized carbonyl oxide (for example, CH_3CHOO), known as a Criegee intermediate, which can then either react with another atmospheric species or decay and, in doing so, produce the hydroxyl radical. Here, we examine the dissociation dynamics of a prototypical Criegee intermediate by characterizing the translational and internal energy distributions of the OH radical products, which reflect critical configurations along the reaction pathway. Experimentally, the kinetic energy release to OH products is ascertained through velocity map imaging. Theoretically, quasi-classical trajectories are performed on a new full-dimensional, *ab initio* potential energy surface. Both experiment and theory show that most of the available energy flows into internal excitation of the vinoxy products. The isotropic angular distribution of OH fragments indicates that dissociation occurs in $\geq$2 ps, in agreement with theory.